Measurements of interaction cross sections for $^{22-35}$Na isotopes

S. Suzuki[1,a], M. Takechi[2], T. Ohtsubo[1], D. Nishimura[3], M. Fukuda[4], T. Kuboki[5], M. Nagashima[1], T. Suzuki[5], T. Yamaguchi[5], A. Ozawa[6], H. Ohishi[6], T. Moriguchi[6], T. Sumikama[3], H. Geissel[2], N. Aoi[7], Rui-Jiu Chen[8], De-Qing Fang[9], N. Fukuda[3], S. Fukuoka[6], H. Furuki[5], N. Inabe[8], Y. Ishibashi[6], T. Ito[1], T. Izumikawa[10], D. Kameda[8], T. Kubo[8], M. Lantz[8], C.S. Lee[5], Yu-Gang Ma[9], M. Mihara[4], S. Momota[11], D. Nagae[6], R. Nishikiori[6], T. Niwa[6], T. Ohnishi[8], K. Okumura[8], T. Ogura[1], H. Sakurai[8], K. Sato[5], Y. Shimbara[1], H. Suzuki[8], H. Takeda[8], S. Takeuchi[8], K. Tanaka[8], H. Uenishi[4], M. Winkler[2], and Y. Yanagisawa[8]

[1] *Graduate School of Science, Niigata University, Niigata 950-2102, Japan*
[2] *Gesellschaft für Schwerionenforschung GSI, 64291 Darmstadt, Germany*
[3] *Department of Physics, Tokyo University of Science, Tokyo 278-8510, Japan*
[4] *Department of Physics, Osaka University, Osaka 560-0043, Japan*
[5] *Department of Physics, Saitama University, Saitama 338-8570, Japan*
[6] *Institute of Physics, University of Tsukuba, Ibaraki 305-8571, Japan*
[7] *Research Center for Nuclear Physics RCNP, Osaka 567-0047, Japan*
[8] *RIKEN Nishina Center for Accelerator-Based Science, Wako, Saitama 351-0198, Japan*
[9] *Shanghai Institute of Applied Physics, Chinese Academy of Sciences, Shanghai 201800, China*
[10] *RI Center, Niigata University, Niigata 950-2102, Japan*
[11] *School of Environmental Science and Engineering, Kochi 782-8502, Japan*

Abstract. Interaction cross sections (σ_I) for $^{22-35}$Na isotopes from the stability line to the vicinity of the neutron drip line have been measured at around 240 MeV/nucleon. The σ_I for $^{33-35}$Na were measured for the first time. Enhancement in cross sections is clearly observed from the systematics for stable nuclei, for isotopes with large mass numbers. From the known values of the nuclear-deformation parameters β_2 of $^{22-31}$Na, these enhancement can be mainly ascribed to the nuclear deformation. Large enhancement in heavier isotopes suggest that these nuclei are strongly deformed. The root-mean-square (RMS) nuclear matter radii were deduced from the σ_I by using Glauber-type calculation. Furthermore, a monotonic growth of the neutron-skin thickness has been deduced with increasing neutron number for Na isotopes.

1 Introduction

The neutron-halo and neutron-skin structures are among the most notable topics in exotic nucei. The observation of large enhancement of nuclear matter radii of unstable nuclei by measuring the σ_I, greatly contributed to discovery of these exotic structures [1, 2]. Therefore, measurement of σ_I is a good tool to study exotic nuclei such as neutron-halo and neutron-skin nuclei. Recently, the region of neutron-rich Ne, Na and Mg isotopes around $N = 20$, known as "island of inversion [3]" has been extensively studied. In this region, in spite of having neutron number around magic number 20, it has been reported that ^{32}Mg and ^{34}Mg are strongly deformed [4, 5], and ^{31}Ne has a neutron-halo structure

---

[a]present address: National Institute of Radiological Sciences, Chiba 263-8555, Japan;e-mail: ssuzuki@nirs.go.jp

[6, 7]. These experimental results also confirm that the magic number 20 vanishes in this region. Recently, we have measured σ_I for Ne isotopes including this region, to suggest the neutron-halo structures of ^{29}Ne and ^{31}Ne from the observed enhancement in σ_I [7]. In the case of Na isotopes, the previous measurement of σ_I at GSI has been done up to ^{32}Na. In the present work, we have measured σ_I for $^{22-35}$Na, including heavier ones $^{33-35}$Na, to study the nuclear structures of Na isotopes located in or beyond the "island of inversion".

2 Experiment

Experiments were performed by using BigRIPS at RIBF, operated by the RIKEN Nishina Center and the Center for Nuclear Study, University of Tokyo. Figure 1 shows a schematic drawing of the experimental setup. A primary beam of 345-MeV/nucleon ^{48}Ca with a typical intensity of 100 pnA was used. Secondary beams of $^{22-35}$Na were produced via projectile fragmentation of ^{48}Ca on Be production targets at the first focal plane (F0). Produced fragments were pre-separated at the first stage of BigRIPS (F1-F3). The Al wedge-shaped degrader was placed at F1. The second stage of BigRIPS (F3-F7) was used to separate and identify the secondary beams. We measured σ_I by using the transmission method. The reaction targets were installed in the F5 (Fig.1). Incident and out-going particles were identified and counted by using detectors that were located upstream side (F3-F5) and downstream side (F5-F7) of the reaction targets, respectively. For particle identification, we used $B\rho$-TOF-ΔE method by using parallel plate avalanche counters (PPAC), plastic-scintilation counters (PL) and ion chambers (IC). These detectors are also shown in Fig. 1. The interaction cross section is deduced from $\sigma_I = -\frac{1}{t} \ln\left(\frac{R}{R_0}\right)$, where t denotes the number of nuclei per unit area in the reaction target. R is the ratio of number of out-going particles divided by that of the incoming particles, and R_0 is the same ratio on a measurement without a reaction target to correct the nuclear reactions in the detectors.
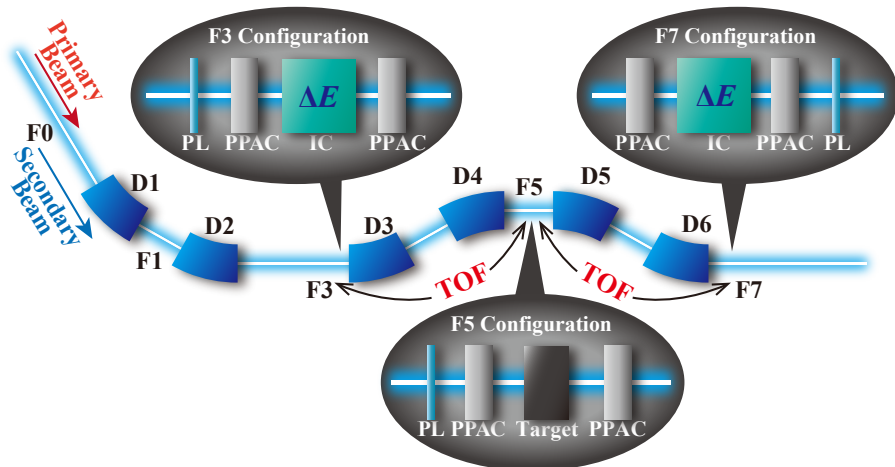
Figure 1. A schematic drawing of the experimental setup. The dipole magnets are indicated as D1-D6. The focal planes are represented as F0-F7. The parallel plate avalanche counters (PPAC), ion chambers (IC) and plastic-scintilation counters (PL) were used to obtain the information of $B\rho$, TOF (Time Of Flight) and ΔE, respectively.

3 Results and discussions

The σ_I for $^{22-35}$Na at 240 MeV/nucleon are plotted as a function of mass number in Fig. 2. In the present work, we measured the σ_I for $^{33-35}$Na for the first time. From mass number 28, the present data deviate from the systematics for stable nuclei as the mass number increases.

The beam energies of Na isotopes in the middle of reaction target were around 240 MeV/nucleon. The σ_I at exact 240 MeV/nucleon were deduced by correcting the energy dependence of nucleon-nucleon interaction cross section (σ_{NN}). The previous data measured at 950 MeV/nucleon in GSI [2] are also plotted in Fig. 2. Plotted values are also corrected to adjust the beam energy to be 240 MeV/nucleon, by using energy dependence of σ_{NN}. The present data are in good agreement with the previous data within the statistical error except for ^{22}Na.
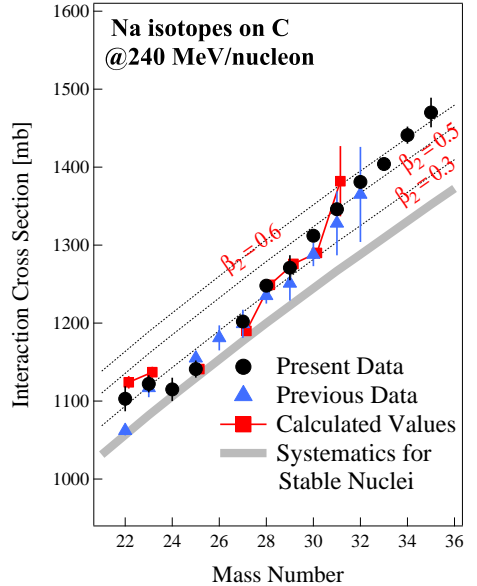
3.1 Effect of nuclear deformation on σ_I

In Fig. 2, the calculated values of σ_I taking into account the quadrupole deformation are shown by the closed squares. The deformation parameters β_2 were deduced from the experimental data of quadrupole moment and reduced transition probability $B(E2)$. Therefore, the calculated values are plotted only for isotopes whose β_2 are known. These calculated values were deduced by using simple geometrical equation of interaction radii, $\sigma_I = \pi[R_I(^{12}C)+R_I(^ANa)]^2$, where $R_I(^{12}C)$ is obtained from the σ_I of $^{12}C + {}^{12}C$ at 240 MeV/nucleon [8], $R_I(^ANa) = R_0 A^{1/3} \sqrt{1 + 5\beta_2^2/4\pi}$ [9]. The R_0 is determined so as to reproduce the σ_I for ^{25}Na whose β_2 is almost zero. The tendency of calculated values reproduces the present data very well. Moreover, the present data suggest that the deformation tends to be larger for isotopes with larger mass numbers.

## 3.2 Neutron-skin thickness of Na isotopes

Figure 2. The observed mass-number dependence of the σ_I for Na isotopes on C targets. The solid circles and the closed triangles show present and previous data [2], respectively. The gray line shows systematics for stable nuclei [7]. The closed squares show the calculated values of the σ_I by using deformation parameters β_2, on the assumption that the systematics for stable nuclei corresponds with $\beta_2 = 0$. The three-dashed lines show the calculated values in the case of β_2 are 0.6, 0.5 or 0.3.

We deduced the root-mean-square (RMS) nuclear matter radii ($\tilde{r}_m$) from present data by using Glauber-type calculation. The density of projectile nucleus is assumed to be Fermi-type, and the diffuseness parameter is fixed to the value of ^{23}Na extracted from elastic electron scattering [10]. In Fig. 3, the mass-number dependence of the RMS nuclear matter radii is shown. The calculated values of Relativistic Mean Field (RMF) theory by Geng et al.[11] are also plotted for comparison. The present data are in good agreement with these calculated values except for $A = 30, 31$. In this RMF theory, the RMS nuclear matter radii of ^{30,31}Na were calculated by assuming that β_2 of these nuclei are almost zero. This result suggests that the shell structures of nuclei located in "island of inversion" are different from those of spherical nucleus.

In Fig. 3, the RMS nuclear proton radii ($\tilde{r}_p$) are also shown. The RMS nuclear proton radii are deduced from the data of electron-scattering and of isotope-shift measurements [12]. For $^{32-35}$Na, we

estimate the RMS nuclear charge radii by extrapolating from the known values [13], because of the lack of experimental data for these nuclei. Figure 4 shows the estimated neutron-skin thickness, where the horizontal axis denotes the difference of the separation energies ($S_p - S_n$). In order to deduce the neutron-skin thickness, we used the following equation, $\tilde{r}_m^2 = \frac{Z}{A}\tilde{r}_p^2 + \frac{N}{A}\tilde{r}_n^2$, where $\tilde{r}_n$ is the RMS nuclear neutron radius. The previous results [2] are also plotted in Fig. 4. The present data are consistent with the previous data. The neutron-skin thickness from the RMF calculation by Geng et al. [11] are also plotted for comparison. Present data are in good agreement with these values in lighter mass region. However in heavier mass region, our results are smaller than the RMF calculation. It could be due to our overestimation of the RMS nuclear charge radii for heavier isotopes. The data in the whole mass range roughly show a linear dependence on $S_p - S_n$, which is in agreement with the RMF calculation.
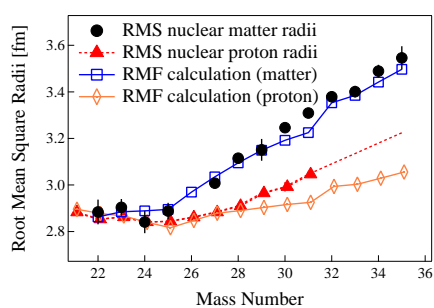
Figure 3. The $\tilde{r}_m$ deduced from present data (solid circles) and the $\tilde{r}_p$ (solid triangles) [12]. The dotted line shows the $\tilde{r}_p$ estimated by the empirical formula for neutron-rich region [13]. The open squares and diamonds show the results of RMF calculation for the $\tilde{r}_m$ and $\tilde{r}_p$[11], respectively.
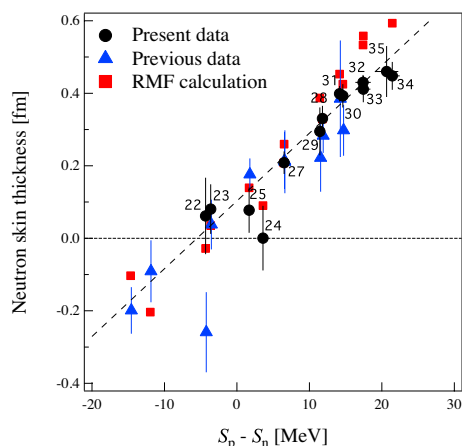
Figure 4. The neutron-skin thickness deduced from present data (solid circles) and previous data (solid triangles) [2]. The closed squares show the RMF calculation values[11].

Acknowledgements

References

[1] I. Tanihata et al., Phys. Rev. Lett. **55**, 2676 (1985).
[2] T. Suzuki et al., Phys Rev. Lett. **75**, 3241 (1995).
[3] E. K. Warburton et al., Phys. Rev. C **41**, 1147 (1990).
[4] T. Motobayashi et al., Phys. Lett. B **346**, 9 (1995).
[5] H. Iwasaki et al., Phys. Lett. B **522**, 227 (2001).
[6] T. Nakamura et al., Phys Rev. Lett. **103**, 262501 (2009).
[7] M. Takechi et al., Phys. Lett. B **707**, 357 (2012).
[8] M. Takechi et al., Phys. Rev. C **79**, 061601 (2009).
[9] L. Chulkov et al. Nuclear Phys. A **603**, 219 (1996).
[10] H. de Vries, C.W. de Jagar, C. de Vries, At. Data Nucl. Data Tables **36**, 495 (1987).
[11] L. S. Geng et al., Nucl. Phys. A **730**, 80 (2004).
[12] E. W. Otten, Treaties on Heavy-Ion Science **8**, 517 (1989).
[13] I. Angeli, At. Data Nucl. Data Tables **87**, 185 (2004).